Preparation of SnO_2 and Nb_2O_5 Supported Vanadium Oxide Catalysts by a Column-Exchange Adsorption Method and Dispersed States of Vanadia Species

Yoshiya KERA* and Takahiro KAWASHIMA
Department of Applied Chemistry, Faculty of Science and Engineering, Kinki University, Higashiosaka, Osaka 577
(Received September 16, 1987)

SnO_2 and Nb_2O_5-supported monolayer or sub monolayer vanadium oxide catalysts were prepared by an impregnation method such as the column-exchange adsorption of oxovanadium ion at various pH(=2, 4, and 7). The deposited states of the vanadia species on SnO_2 and Nb_2O_5 surfaces were examined by ESR spectrometry using V^{4+} ion as a probe. The catalytic features were studied by measuring the 2-propanol decomposition rate as a test reaction. The deposited states of the vanadia species differed to a small extent between SnO_2 and Nb_2O_5 carriers depending upon the difference in the symmetry of the surface field. The deposited states, however, did not vary with pH upon impregnation, although the amounts of vanadium oxide deposited (coverage, θ) were much affected by the pH. The activation energy (E_a) for the dehydration of 2-propanol over these catalysts was linearly related to the reciprocal of the coverage ($1/\theta$). When both curves were extended to $1/\theta=0$, they crossed at around 5—6 kcal·mol^{-1} which was the minimum value, although the inclination differed largely between the carriers. This low activation energy was regarded as an intrinsic value that was caused by the multi-layered vanadium oxide deposited on the carriers. Through the discussion it is clearly shown that the most effective catalyst, a monolayer catalyst, was prepared on impregnation at pH=2 and the vanadia species were dispersed widely, keeping a weak interaction with the SnO_2 and Nb_2O_5 surfaces.

A column-exchange adsorption method [1] has been reported as an effective method for preparing vanadium oxide monolayer catalysts that have a superior activity and the selectivity for hydrocarbon oxidations, especially in titania-supported vanadia catalysts.[2-4] Previously the deposited state of a monolayer or sub monolayer vanadium oxide was shown to depend greatly upon the crystalline symmetry of the support. This in turn depends upon the crystal field symmetry around the cation on the surface. ESR analysis has been applied to vanadia deposited on rutile and anatase[5] by such an exchange-adsorption method. Many investigators have studied the binary V_2O_5–SnO_2 catalyst system because it has a high activity and selectivity for ammoxidation and various hydrocarbon oxidations.[6-13] The effect of pH on vanadium oxide monolayer catalysts deposited on SnO_2 (the crystal structure of which belongs to rutile type[14]) were examined by the column-exchange adsorption method. We also prepared vanadium oxide monolayer catalysts deposited on Nb_2O_5 which have a V_2O_5 type crystal structure.[15] We were interested specially in the interaction between vanadia species and Nb_2O_5 surfaces and in comparing the result with those of SnO_2 and titania (rutile and anatase). Recently many people have payed attention to Nb_2O_5 as a catalyst carrier bacause it shows a higher Strong-Metal-Support Interaction (SMSI) than TiO_2 or ZrO_2 carriers.[16]

ESR analysis for V^{4+} ion showed that vanadia deposited on SnO_2 and Nb_2O_5 appeared to interact more weakly with those carrier surfaces than TiO_2 (rutile). The interaction was similar in extent to that of TiO_2 (anatase). Of special interest is the linear relation between the apparent activation energy(E_a) for 2-propanol decomposition on the catalysts and the reciplocal of the surface coverage(θ) of the vanadia species. The E_a vs. $1/\theta$ curves for V_2O_5/SnO_2 and Nb_2O_5, which were extrapolated to $1/\theta$ both gave the lowest E_a=5—6 kcal·mol^{-1}. This should be regarded as the intrinsic activation energy for 2-propanol decomposition over the multi-layered vanadium oxide on SnO_2 and Nb_2O_5. Such a low value appeared to arise only from the vanadium oxide dispersed widely on the carrier surface with a weak interaction.

Experimental

1) **Materials and Preparation Procedures.** Four grams of Nb_2O_5 powder (Nakarai Chem. Co., Ltd., guaranteed grade) was packed into a glass column (o.d.=15 mm). About 0.5 wt% of NH_4VO_3 (Kanto Chem. Co., Ltd., guaranteed grade) aqueous solution, the pH of which were exactly adjusted at 2, 4, and 7 by adding HNO_3 and aqueous ammonia, were poured into the column to make the oxovanadium ion adsorb. Each 3 ml of the effluent solution was collected to measure the changes in the pH and the concentration of oxovanadium ion (V-ion) while passing through the column.

For the SnO_2 carrier (Kanto Chem. Co., Ltd., guaranteed grade), about 4 g were packed into the column; the NH_4VO_3 solution was added until both the pH and V-ion concentration had recovered to the original values. Those pH and V-ion concentrations were determined by the use of a pH-meter, TOA model HM-7B and the usual Mohr-titration method, respectively. After the adsorption, the samples were dried at 110 °C for 8 h, and then calcined at 400 °C for 2 h in order to prepare Nb_2O_5 and SnO_2 supported vanadium oxide catalysts, V_2O_5/Nb_2O_5 and V_2O_5/SnO_2.

2) **Measurements and Computer Simulation.** The surface areas of V_2O_5/Nb_2O_5 and SnO_2 were determined by N_2 gas adsorption at 77 K according to a convenient method.[17] The deposited states of the vanadia species were examined by ESR spectrometry. The ESR spectrometer used was a Nippon Denshi Model JES-PE (X-band, 9.3 GHz and 100 kHz modulation). Computer simulation of the ESR spectrum was performed using an IBM 4381 system. The catalytic activities for 2-propanol decomposition, as a test reaction, were measured in a closed circulation system (ca. 0.5 dm^3) connected directly to the gaschromatograph with a Porapac-Q column (1 m). 20 mg of the catalysts were spread widely over the bottom of the vassel and preheated at the reaction temperature in air for one hour before the reaction. The vessel containing 2-propanol was cooled by an ice-water bath during the reaction in order to maintain the vapor pressure constant at 8.4 mmHg (1 mmHg≈133.322 Pa). The intensity of the GC-peak of the main product, (that was confirmed to be propylene) was measured at intervals of 2 min. The decomposition rate was determined from the intensity change for the initial 20 min. The reaction temperature was controlled within ±0.5 °C in the range 270—350 °C.

Results

1) **The Amounts of Vanadium Oxide Deposited on SnO_2 and Nb_2O_5 Carriers.** When the NH_4VO_3 aqueous solutions with different pH were poured into the glass column packed with SnO_2 carrier, the pH and vanadium ion (V-ion) concentration of the effluent solution varied as shown in Fig. 1. The pH initially increased from 2 to about 4 or more in a run of pH=2 and increased only slightly in a run at pH=4, while in a run at pH=7 it decreased to near 6. The pH finally returned to the original values in all runs. Accompanied by the pH-changes, the V-ion concentrations initially decreased and then gradually recovered to the original values. The amounts of the adsorbed vanadium ion were estimated, based on these V-ion concentration vs. effluent-volume cruves. The adsorbed amounts of oxovanadium ion, which were estimated on the assumption that they were deposited in the form of V_2O_5, are given in the 3rd and 4th column of Table 1 (in units of $mg(V_2O_5)\cdot g\text{-carrier}^{-1}$ and $mg(V_2O_5)\cdot m^{-2}$, respectively). The surface area and surface coverage are also given in the 2nd and 5th column in Table 1, respectively. The coverage was estimated on the assumption that the V–O–V network of V_2O_5 extends two-dimensionally on the SnO_2 carrier and the V–O bond distance is 2.0 Å.[18]

With respect to the Nb_2O_5 carrier, the changes in the pH and the V-ion concentration of the effluent solutions are shown in Fig. 2. The pH change is small in all pH runs. The V-ion concentration initially

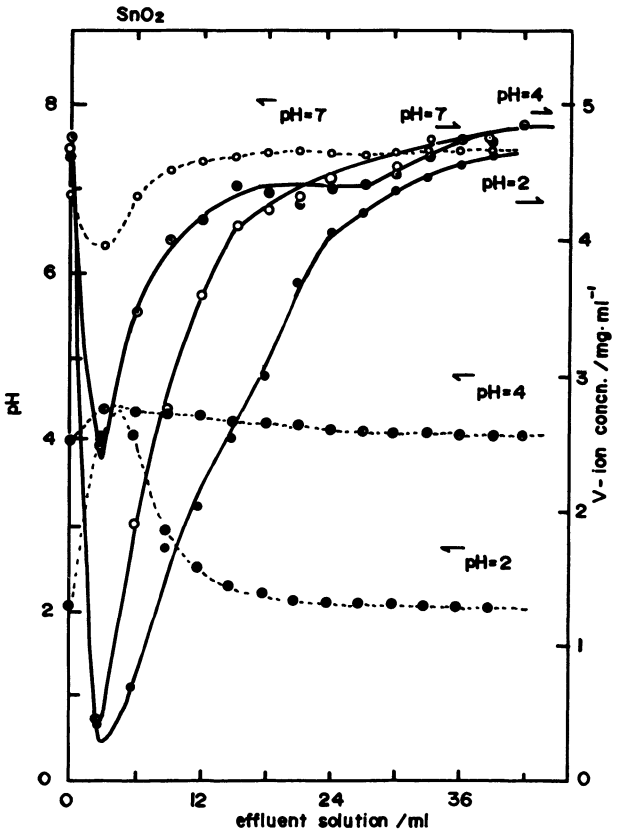

Fig. 1. The variations of pH and vanadium ion concentration in ammonium metavanadate effluent solution during passing through SnO_2-packed column for various pH runs. ----: pH change and —: V-ion concentration change.

Table 1. Surface Areas, the Amounts of Vanadium Oxide Deposited (Reduced to V_2O_5), and the Surface Coverages of V_2O_5/SnO_2 and V_2O_5/Nb_2O_5

Catalyst	Surface area	Deposited amounts		Surface coverage
	$m^2\cdot g^{-1}$	$mg(V_2O_5)\cdot g\text{-car.}^{-1}$	$mg\cdot m^{-2}$	(θ)
SnO_2 carrier	32	—	—	—
V_2O_5/SnO_2 (pH=2)	36	29	0.80	0.42
V_2O_5/SnO_2 (pH=4)	39	10	0.25	0.14
V_2O_5/SnO_2 (pH=7)	35	15	0.42	0.22
Nb_2O_5 carrier	3.9	—	—	—
V_2O_5/Nb_2O_5 (pH=2)	3.6	9.5	2.6	1.4
V_2O_5/Nb_2O_5 (pH=4)	3.4	5.9	1.7	0.90
V_2O_5/Nb_2O_5 (pH=7)	3.7	1.4	0.38	0.19
V_2O_5 powder	8.5	—	—	—

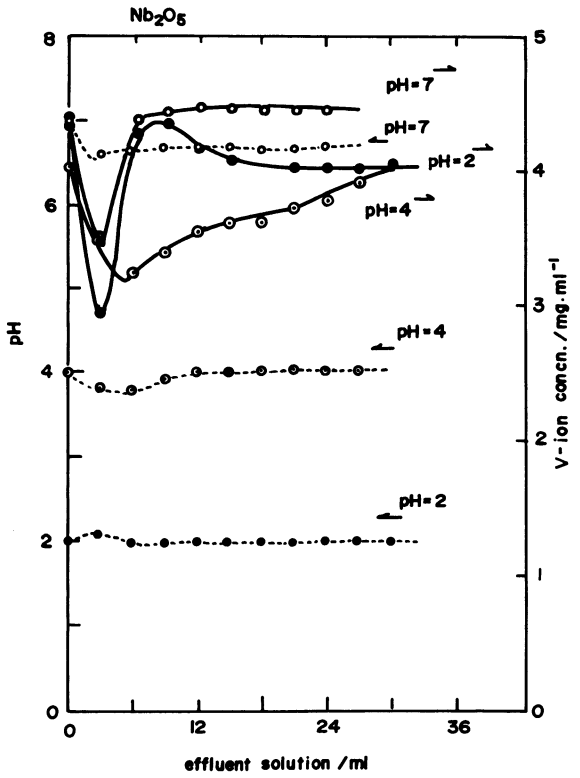

Fig. 2. The variations of pH and vanadium ion concentration in ammonium metavanadate effluent solution during passing through Nb_2O_5-packed column for various pH runs. ----: pH change and —: V-ion concentration change.

decreases slightly relative to the case of SnO_2 because of the small surface area. The concentration curve does not fully return to the original value except for a run at pH=7. The adsorbed amounts of vanadium ion were similarly estimated as given in the 3rd and 4th column of Table 1. The surface areas and the coverage are also given in the 2nd and 5th column of Table 1, respectively.

2) **ESR Spectra of V(IV) Ion on V_2O_5/SnO_2 and Nb_2O_5.** The ESR spectrum of the supported vanadia catalysts did not basically differ with the pH upon impregnation. The ESR spectra for V_2O_5/SnO_2 impregnated at pH=2 and 7, which were measured at 77 K after the evacuation at room temperature, are illustrated in Fig. 3-a and b, respectively. The spectrum for V_2O_5/SnO_2(pH=7), which was measured at 77 K after the evacuation at 400 °C, is shown in Fig. 3-c. The spectrum is considered to contain 8 hf-lines due to the ^{51}V-nucleus (I=7/2). After heat treatment at 400 °C, however, the spectrum varies in a complex manner; the other ESR species are added to the original one. V_2O_5/SnO_2 (pH=2) shows a composite spectrum even upon pretreatment at room temperature.

The ESR spectra for V_2O_5/Nb_2O_5 impregnated at pH=2 and 7, which are measured at 77 K after evacuation at room temperature, are illustrated in Figs. 4-a and b. The spectrum of V_2O_5/Nb_2O_5(pH=2), the surface coverage (θ) of which is larger than unity, shows specially unresolved hfs upon evacuation at

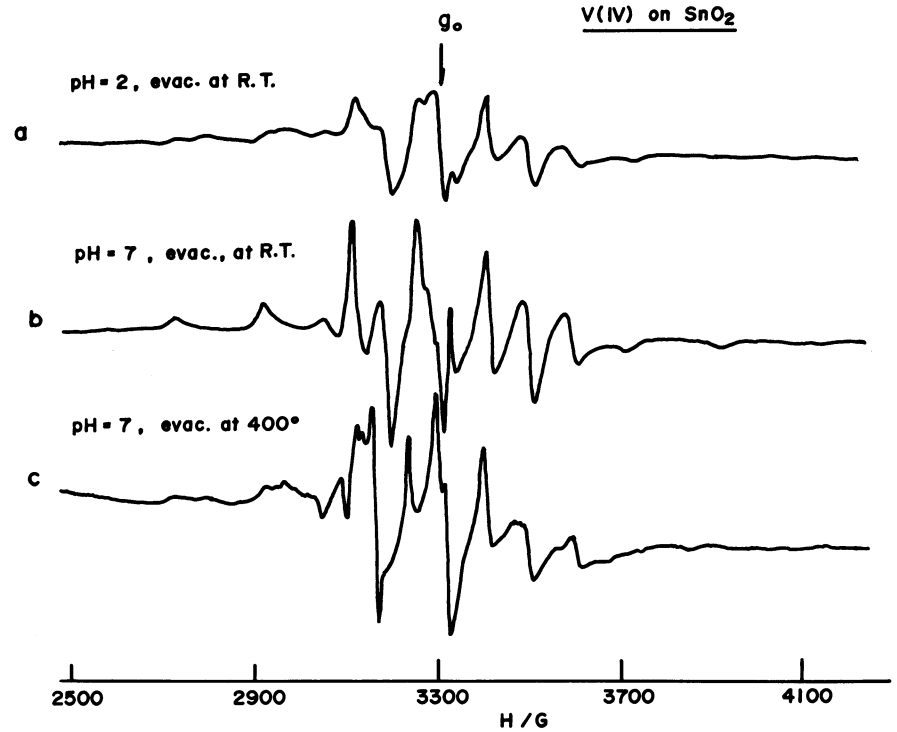

Fig. 3. ESR spectra for V(IV) ion on V_2O_5/SnO_2 prepared at pH=2 and 7. a: on V_2O_5/SnO_2 (pH=2), which was measured at 77 K after evacuating at room temperature, b: on V_2O_5/SnO_2 (pH=7), which was measured at 77 K after evacuating at room temperature, and c: on V_2O_5/SnO_2 (pH=7) measured at 77 K after evacuating at 400 °C.

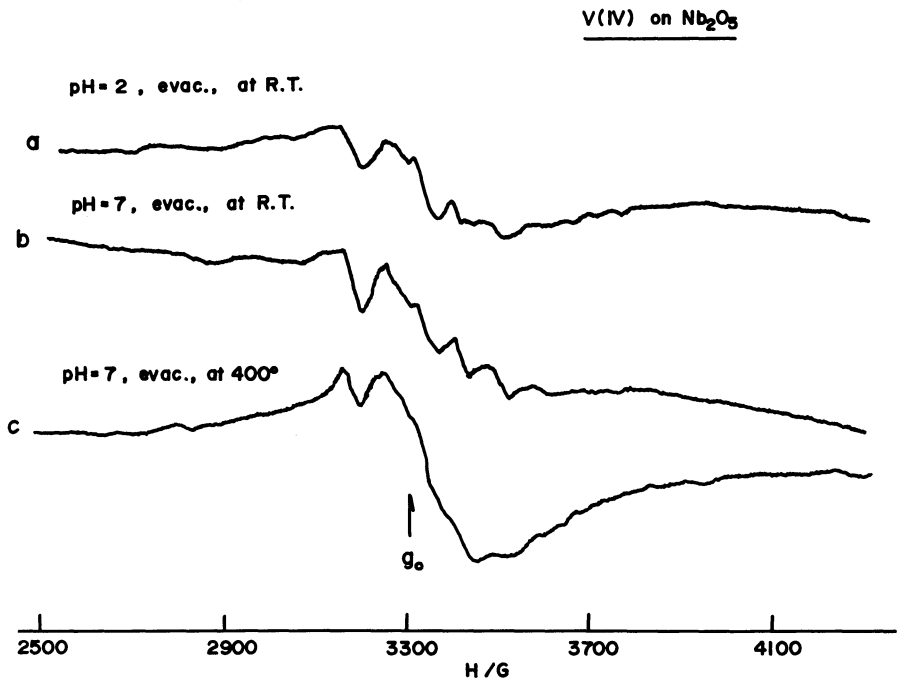

Fig. 4. ESR spectra for V(IV) ion on V_2O_5/Nb_2O_5 prepared at pH=2 and 7. a: on V_2O_5/Nb_2O_5 (pH=2) which was measured at 77 K after evacuating at room temperature, b: on V_2O_5/Nb_2O_5 (pH=7) which was measured at 77 K after evacuating at room temperature, and c: on V_2O_5/Nb_2O_5 (pH=7) which was measured at 77 K after evacuating at 400 °C.

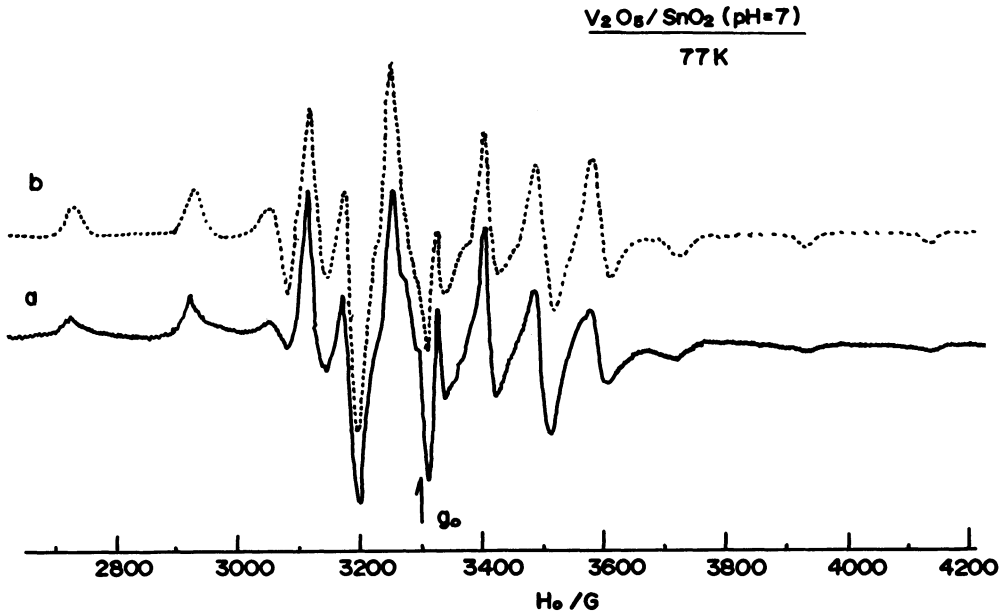

Fig. 5. The ESR spectrum for V_2O_5/SnO_2 (pH=7) and the best fit spectrum simulated. —: observed and ----: simulated.

room temperature. V_2O_5/Nb_2O_5(pH=7) shows a relatively clear hfs upon evacuation at room temperature, but after evacuation at 400 °C the hfs completely disappeared and a very broad spectrum appeared.

A computer simulation was applied to the spectra of Figs. 3-b and 4-b which were measured for V_2O_5/SnO_2 and Nb_2O_5 impregnated at pH=7 at 77 K after evacuation at room temperature. The first derivative curve was calculated according to the usual simulation method at intervals of 10 G (1 G=10^{-4} T) in a magnetic field of 2600—4300 G, as described previously.[5] The intensity of the microwave absorption at each resonance field was obtained by numerical inte-

Table 2. The Best Fitting Parameters Used for Simulating the ESR Spectra of V(IV) Ion on V_2O_5/SnO_2 and V_2O_5/Nb_2O_5 Catalysts Evacuated at Room Temperature

Catalyst	Species	g value		A value		Line width
		$g_{//}$	$g_{\perp}$	$A_{//}$/G	$A_{\perp}$/G	d/G
V_2O_5/SnO_2	V(IV)	1.9265	1.9807	200.5	74.0	27
V_2O_5/Nb_2O_5	V(IV)	1.9100	1.9780	200.0	70.0	40

Table 3. Arrhenius Parameters of 2-Propanol Decomposition over V_2O_5/SnO_2 and V_2O_5/Nb_2O_5 Catalysts Impregnated at pH=2, 4, and 7

Catalyst	$\log V_o$ molecules·m^{-2} s^{-1}	E_a kcal·mol^{-1}
SnO_2 carrier	23.7	16.2
V_2O_5/SnO_2 (pH=2)	21.3	9.6
V_2O_5/SnO_2 (pH=4)	24.0	17.0
V_2O_5/SnO_2 (pH=7)	22.8	13.0
Nb_2O_5 carrier	26.4	20.0
V_2O_5/Nb_2O_5 (pH=2)	22.0	7.2
V_2O_5/Nb_2O_5 (pH=4)	22.2	8.0
V_2O_5/Nb_2O_5 (pH=7)	25.9	18.2

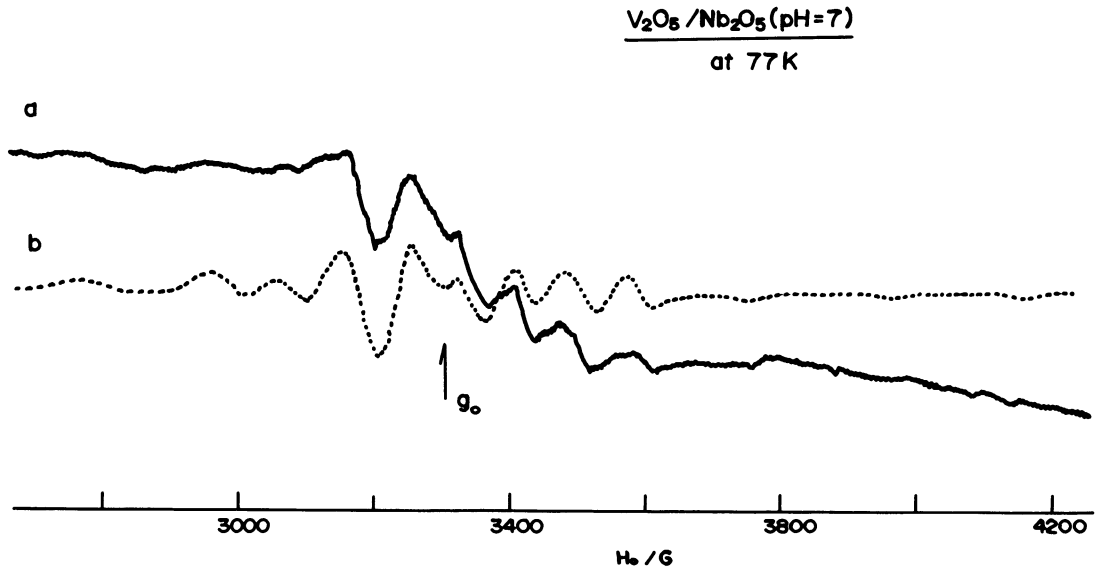

Fig. 6. The ESR spectrum for V_2O_5/Nb_2O_5 (pH=7) and the best fit spectrum simulated. —: observed and ----: simulated.

grations at intervals of 1.5° to θ and ϕ for all directions under the assumption of a Gaussian shape function and 27 G of the half width for V_2O_5/SnO_2 and 40 G for V_2O_5/Nb_2O_5. The best-fit parameters are given in Table 2 and the simulated spectra are shown by the broken line in Figs. 5-b and 6-b.

3) **Decomposition Rates of 2-Propanol over V_2O_5/SnO_2 and Nb_2O_5.** The reaction rates of 2-propanol decomposition over the SnO_2 and Nb_2O_5-supported vanadium oxide catalysts were determined from changes in the GC-peak intensity for the produced propylene in the temperature range 270—350 °C. Arrhenius plots for the initial mean rates, thus obtained, are summarized in Fig. 7(Arrhenius relation: $V=V_o\exp(-E_a/RT)$ and $\log V=\log V_o-E_a/RT$). Arrhenius parameters, $\log V_o$ and E_a, estimated from those plots, are given in Table 3. The minimum activation energy was found to be 7.2 kcal·mol^{-1} for V_2O_5/Nb_2O_5 prepared at pH=2, while the maximum was 18.2 kcal·mol^{-1} for V_2O_5/Nb_2O_5 prepared at pH=7. The activation energy tends to decrease with the amounts of vanadium oxide deposited in any series of catalysts.

The reaction rates in units of molecules·m^{-2}·s^{-1} and molecules·mg$(V_2O_5)^{-1}$·s^{-1}, which were estimated at 300 °C in Fig. 7, are shown in Figs. 8 and 9, respec-

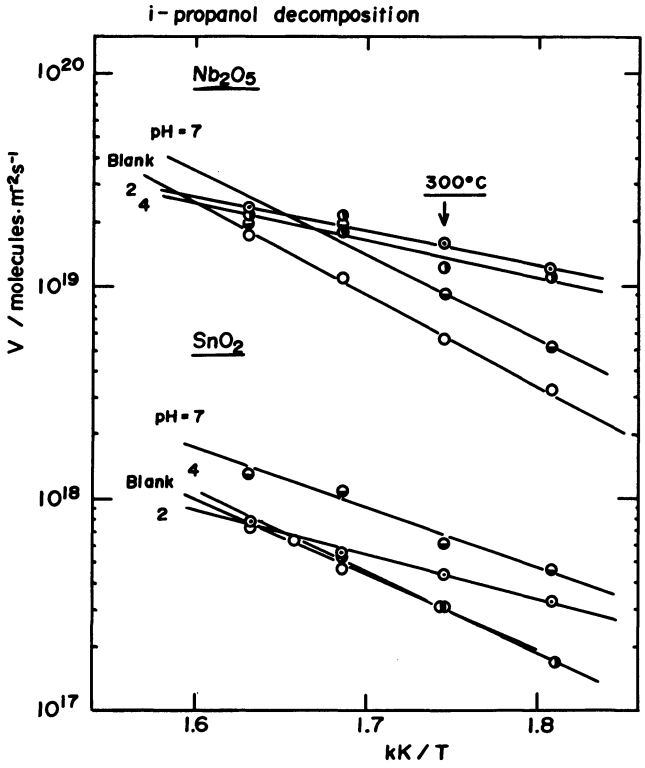

Fig. 7. Arrhenius plots for the 2-propanol decomposition rates over V_2O_5/SnO_2, Nb_2O_5 prepared at various pH and carrier themselves.

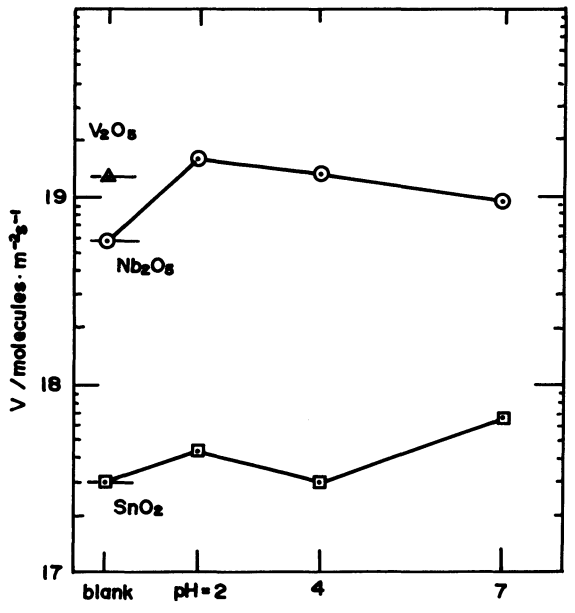

Fig. 8. Comparison of the activity per m^2 and per second for 2-propanol decomposition among V_2O_5 powder, the carrier themselves, and the supported vanadium oxide catalysts at 300°.

tively. In Fig. 8, the activity per m^2 of V_2O_5 powder is higher than those of the carriers, Nb_2O_5 and SnO_2, and the activity is accelerated 2—3 times in V_2O_5/Nb_2O_5 catalysts and twice or less in V_2O_5/SnO_2 relative to the carrier themselves. In Fig. 9, the activity per

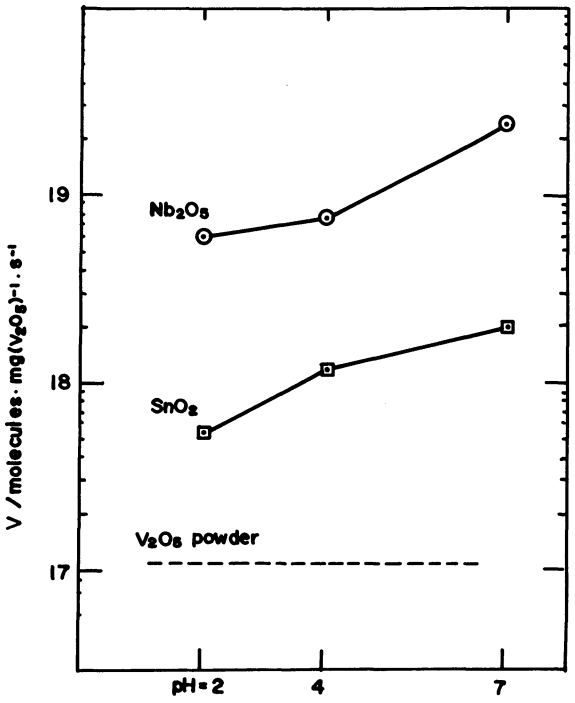

Fig. 9. Comparison of activity per $mg(V_2O_5)$ and per second for 2-propanol decomposition among V_2O_5 powder and the supported catalysts at 300°C.

$mg(V_2O_5)$ generally increases with the pH upon the impregnation and the maximum activity was attained at pH=7 in both carriers. It should be specially noted that the activity is 50—200 times higher in V_2O_5/Nb_2O_5 and 5—20 times higher in V_2O_5/SnO_2 than that of V_2O_5 powder itself. Thus, it is evident that the vanadia species spread widely over the carrier surfaces.

Discussion

Deposited States of Vanadium Oxide on SnO_2 and Nb_2O_5. The deposited states of vanadium oxide on titania (rutile and anatese) have been successfully studied through the analysis of the ESR spectra using the surface V(IV) ion as a probe. The deposited state is greatly affected by the crystal structure of the original carrier; the vanadia species on rutile differed from that on anatase.[5] SnO_2 belongs to the rutile type structure, although the radius ratio $r_{cation}:r_{anion}$ is slightly larger in $SnO_2(r_c/r_a=0.53)$ than in rutile (0.45).[14] Thus, we can also estimate the d-orbital splitting of V(IV) ion from the g-value by Eq. 1.[19]

$$g_{//} = g_o + 8\lambda/\Delta \text{ and } g_{\perp} = g_o + 2\lambda/\delta \quad (1)$$

where Δ and δ are the crystal field splitting constants and λ the spin-orbit coupling constant which is assumed reasonably to be 250 cm^{-1}.[20]

With respect to V(IV) ion doped into SnO_2 crystalline lattice, the coordination model and d-orbital splitting that was estimated from a reported

g-value[21] by Eq. 1 are shown in Fig. 10-a. For V(IV) ion in the vanadia species deposited on SnO_2, the $g_\perp$ component in Table 2 is large and the $g_{//}$ small ralative to those for the doped sample. The differences in the g-values indicate that the d-orbital splitting Δ, decreases and the δ increases when the V(IV) ion located in the inner bulk is brought to the top of the surface. A similar change was found in the titania-vanadia system:[5] Previously, we showed that the field symmetry around the V(IV) ion replacing the Ti ion site on the rutile surface was similar to that around the V(IV) ion placed in a distorted square pyramidal field. The V(IV) ion doped into a rutile crystal was subject to an octahedral field. Thus, accompanied by removing the V(IV) ion from inner bulk to the top of the rutile surface, the crystal field around V(IV) ion changes from octahedral to a distorted square pyramid. The coordination model and the d-orbital splittings for V_2O_5/SnO_2 are shown analogously in Fig. 10-b. However, V(IV) ion placed on an SnO_2 surface is subject to a weaker field than that on rutile, because the ratio of r_c/r_a is larger in SnO_2 than TiO_2.[14] In fact, the splitting constant, Δ and δ, for V(IV) ion deposited on SnO_2 are smaller than those on rutile (Δ=38 and δ=26 kcm^{-1}).[5] Moreover, the extent of the interaction between vanadia species and carrier surfaces can be compared, based on the hf-coupling constant for the V(IV) ion as a probe, as previously pointed out;[5] since $A_{//}$ and $A_\perp$ for V_2O_5/SnO_2 are 200.5 and 74 G, respectively, while those for $V_2O_5/R\text{-}TiO_2$ 173.1 and 55 G, the interaction for V_2O_5/SnO_2 is understood to be weaker than that for $V_2O_5/R\text{-}TiO_2$. The extent of the hf-splittings of V_2O_5/SnO_2 is similar to those of $V_2O_5/A\text{-}TiO_2$ described in the previous paper(Δ=22 and δ=24 kcm^{-1}), in which the V(IV) ion was assumed to be placed only near the Ti ion vacant site.[5]

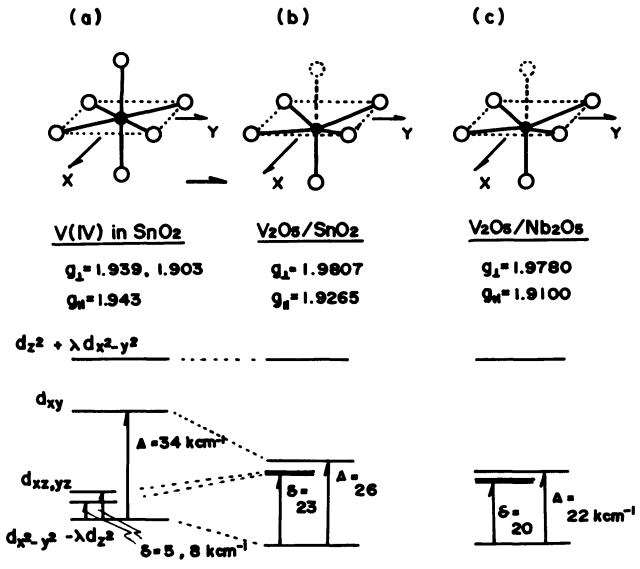

Fig. 10. Coodination model and crystal field splitting for the surface V(IV) ion in V_2O_5/SnO_2 and Nb_2O_5. Analysis for the data of V(IV) ion doped in SnO_2 lattice[21] is shown in (a) for comparison.

The spectrum for V_2O_5/SnO_2 sharpens considerably but remains complicated, after the evacuation at 400 °C, as illustrated in Fig. 3-c. Some reduced vanadia species might be formed by such evacuation treatment and spread over the surface without interacting with each other. Thus, no reduced phase was detected even upon the high temperature evacuation.

Nb_2O_5 belongs to a V_2O_5 type crystal but the oxygen ion coordination around the Nb ion is closer to octahedral symmetry than that of V_2O_5, because the ionic radius of Nb(1.43 A) is larger than that of V(1.32 A).[15] The g-value for the V(IV) ion on Nb_2O_5 surface is almost the same as on an SnO_2 surface, and also close to that for the V_2O_5 inner lattice.[22] Thus, the coordination model and the splitting constants are close to those of V_2O_5/SnO_2, as Fig. 10-c shows. When the V_2O_5/Nb_2O_5 catalyst was evacuated at 400 °C, the spectrum with hfs changed to a broad one as Fig. 4-c illustrated. The broadening might be caused by a dipole-dipole interaction between a reduced vanadia species produced by such a high temperature evacuation.

Catalytic Properties of V_2O_5/SnO_2 and Nb_2O_5. A good compensation relation was found between log V_o and E_a for 2-propanol decomposition over the titania-supported vanadia catalysts, $V_2O_5/R\text{-}$ and $A\text{-}TiO_2$, prepared by the column-exchange adsorption of oxo-vanadium ion under different pH(=2, 4, and 7).[5] Based on such a compensation relation,[23] we could discuss the best conditions for the catalyst preparation. A compensation relation also holds between log V_o and E_a in Table 3 for the catalysts , V_2O_5/SnO_2 and Nb_2O_5, impregnated at different pH(=2, 4, and 7), as shown in Fig. 11. The lowest activation energy was obtained for both SnO_2 and Nb_2O_5 carriers on impregnation at pH=2. The most desirable conditions, thus, is impregnation at pH=2.

E_a tends to decrease with increase in the coverage, θ, as indicated previously. In fact, the E_a vs. $1/\theta$ plot gives a good linear curve, as shown in Fig. 12. The inclination of the curve for SnO_2 differs to some extent from that for Nb_2O_5, but both curves cross at around E_a=5—6 kcal·mol^{-1} upon extrapolation to $1/\theta$=0. The E_a value should correspond to such activation energy as caused by the multilayered vanadium oxide piled on SnO_2 and Nb_2O_5 surfaces; it might indicate an intrinsic activation energy for pure vanadium oxide crystallite. We have never found any linear relation between E_a and $1/\theta$ in vanadia-titania[5] and -zirconia[24] systems. With these carriers, not only the coverage (θ) but also the deposited states would be affected by the pH upon preparation, although the difference in the deposited states could never be detected by ESR-measurement.

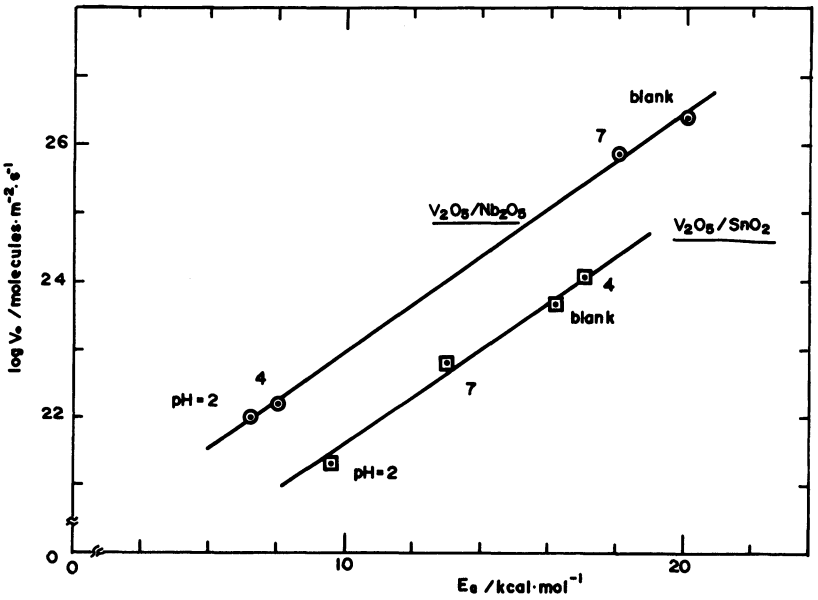

Fig. 11. Relationship between the pre-exponential factor (log V_o) and the activation energy (E_a) for 2-propanol decomposition over the SnO_2- and Nb_2O_5-supported vanadium oxide catalysts.

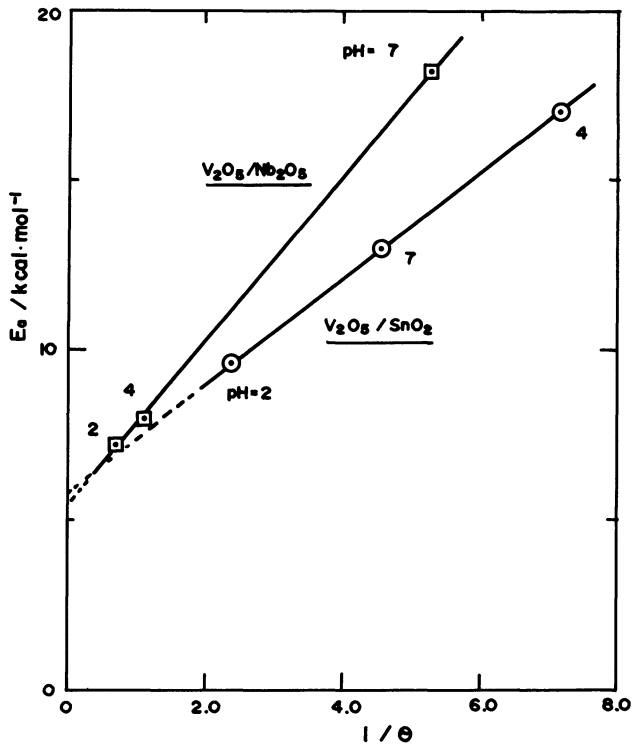

Fig. 12. Relationship between the activation energy and the reverse of the surface coverage ($1/\theta$) of vanadium oxide dispersed on SnO_2 and Nb_2O_5 carriers, see text in detail.

Hernadi et al.[12] showed that the maximum selectivity for 1-butene oxidation was obtained in the composition interval $3:1<V_2O_5:SnO_2<2:1$. Ai[9] showed that the highest activity was obtained for the V_2O_5–SnO_2 catalyst with atomic ratio V:Sn=1:1 and it was the most effective composition for production of maleic anhydride. Andersson[6] suggested in the study on ammonxidation of 3-methylpyridine on V_2O_5/SnO_2 that the catalyst with both V_2O_5 and V_6O_{13} phases is especially active and selective and that the effective catalyst has the composition $V_{0.03}Sn_{0.97}O_2$, in which the V=O bond is weakened by the incorporation of Sn^{4+} ion into the V_2O_5 lattice. Hauffe et al.[10] gave a similar suggestion for the effective working state of various metal oxide supported V_2O_5 catalysts. These authors were also concerned with the fused binary V_2O_5–SnO_2 catalyst, and the effective species were suggested to be formed by the incoporation of Sn^{4+} ion into vanadium oxide lattice. Ono et al.[11] investigated the rates of oxidation of C_3H_6, C_2H_4, C_3H_8, and CO over V–Sn oxides of various compositions. The rates showed two maxima at V/Sn= 2/1 and 1/8. Their ESR, IR, and X-ray measurements suggested that the former rate maximum arises from the formation of an amorphous compound and the latter is associated with the presence of a V^{4+} ion dissolved into SnO_2.[21,25] We have had no evidence for either the incorporations of Sn^{4+} and Nb^{5+} ions into the vanadia species or of V^{4+} ion into SnO_2 and Nb_2O_5 carriers. With the present impregnated catalysts, since the vanadia species were clearly shown to be deposited on SnO_2 and Nb_2O_5 surfaces in the same manner as vanadium ion (V^{4+}) is placed near the Sn^{4+} and Nb^{5+} vacant sites. However we can not directly compare the surface state with those of their fused catalysts. However, the V–O bond can surely be considered to be weakened in such vanadia species as are interacting with the carrier surface, even though quite weakly, as

was discussed for the titania–vanadia system in the previous paper.[5]

Finally, it should be noted that the weak interaction of vanadia species with Nb_2O_5 contrasts with the SMSI in metal supported Nb_2O_5 catalyst.[16] These V_2O_5/SnO_2 and Nb_2O_5 catalysts will be tested for ammoxidation and hydrocarbon oxidation in the near future.

References

1) F. Roozeboom, T. Fransen, P. Mars, and P. J. Gellings, *Z. Anorg. Allg. Chem.*, **449**, 25 (1979); F. Roozeboom, J. Medema, and P. J. Gellings, *Z. Phys. Chem., NF*, **111**, 215 (1978); F. Roozeboom, P. D. Cordingely, and P. J. Gellings, *J. Catal.*, **68**, 464 (1981); F. Roozeboom, M. C. Mittelmeijer-Hazeleger, J. A. Moulijn, J. Medema, V. H. J. de Beer, and P. J. Gellings, *J. Phys. Chem.*, **84**, 2783 (1980).

2) G. C. Bond and K. Brukman, *Faraday Discuss. Chem. Soc.*, **72**, 235 (1981); G. C. Band and P. Konig, *J. Catal.*, **77**, 309 (1982).

3) M. Rusiecka, B. Grzybowska, and M. Gasior, *Appl. Catal.*, **10**, 101 (1984).

4) I. E. Wachs, R. Y. Saleh, S. S. Chan, and C. C. Chersich, *Appl. Catal.*, **15**, 339 (1985); R. Y. Saleh, I. E. Wachs, S. S. Chan, and C. C. Chersich, *J. Catal.*, **98**, 102 (1986).

5) Y. Kera and Y. Matsukaze, *J. Phys. Chem.*, **90**, 5752 (1986); Y. Kera, T. Inoue, and Y. Matsukaze, *Bull. Chem. Soc. Jpn.*, **61**, 761 (1988).

6) A. Andersson, *J. Catal.*, **69**, 465 (1981).

7) K. L. Madhok, *React. Kinet. Catal. Lett.*, **25**, 159 (1984).

8) P. J. Pomonis and J. C. Vickerman, *J. Chem. Soc., Faraday Discuss.*, **72**, 247 (1981); *J. Catal.*, **90**, 305 (1984).

9) M. Ai, *J. Catal.*, **40**, 318 (1975).

10) K. Hauffe and H. Raveling, *Ber. Bunsenges. Phys. Chem.*, **84**, 912 (1980).

11) T. Ono, Y. Nakagawa, and Y. Kubokawa, *Bull. Chem. Soc. Jpn.*, **54**, 343 (1981); T. Ono and Y. Kubokawa, *Bull. Chem. Soc. Jpn.*, **55**, 1748 (1982).

12) K. Hernadi, J. Halasz, K. Varga, and P. Fejes, *Acta Phys. Chem.*, **30**, 97 (1984).

13) Yu. D. Panakratiev, L. N. Kurina, T. V. Lazareva, and S. P. Rabota, *React. Kinet. Catal. Lett.*, **27**, 173 (1985).

14) W. Huckel, "Structural Chemistry of Inorganic Compounds(II)," Elsevior Sci., New York (1951), p. 581.

15) R. Kiriyama and H. Kiriyama, "Structural Inorganic Chemistry," 2nd ed, Kyoritsu, Tokyo (1964). p. 142.

16) K. Tanabe and T. Iizuka, *Hyomen*, **23**, 471 (1985).

17) V. M. Samoilov and A. N. Ryabov, *Kinet. Katal.*, **19**, 250 (1978).

18) A. Bystrom, K. Wilhelmi, and O. Brotzen, *Acta Chem. Scand.*, **4**, 1119 (1950).

19) B. A. Goodman and J. B. Bayer, *Advan. Inorg. Chem. Radiochem.*, **13**, 135 (1970).

20) G. C. Pake, "Paramagnetic Resonance," W. A. Benjanin, New York (1962).

21) C. Kikuchi, I. Chen, W. H. From, and P. B. Dorain, *J. Chem. Phys.*, **42**, 181 (1965).

22) Y. Kera and K. Kuwata, *Bull. Chem. Soc. Jpn.*, **52**, 1268 (1979).

23) Y. Kera and M. Negoro, *J. Catal.*, **99**, 198 (1986).

24) Y. Kera and T. Kamada, unpublished data.

25) P. H. Kasai, *Phys. Lett.*, **7**, 5 (1963).